Monthly Notices
of the
ROYAL ASTRONOMICAL SOCIETY

Mon. Not. R. Astron. Soc. **420,** 1848–1860 (2012) doi:10.1111/j.1365-2966.2011.19779.x

Intrinsic disc emission and the soft X-ray excess in active galactic nuclei

Chris Done,[1⋆] S. W. Davis,[2] C. Jin,[1] O. Blaes[3] and M. Ward[1]

[1]*Department of Physics, University of Durham, South Road, Durham DH1 3LE*
[2]*CITA, University of Toronto, 60 George Street, Toronto, ON M5S 3H8, Canada*
[3]*Department of Physics, Broida Hall, UCSB, CA 93106-9530, USA*

Accepted 2011 September 6. Received 2011 September 6; in original form 2011 July 27

ABSTRACT

Narrow-line Seyfert 1 (NLS1) galaxies have low-mass black holes and mass accretion rates close to (or exceeding) Eddington, so a standard blackbody accretion disc should peak in the extreme ultraviolet. However, the lack of true absorption opacity in the disc means that the emission is better approximated by a colour temperature corrected blackbody, and this colour temperature correction is large enough (∼2.4) that the bare disc emission from a zero spin black hole can extend into the soft X-ray bandpass. Part of the soft X-ray excess seen in these objects must be intrinsic emission from the disc unless the vertical structure is very different to that predicted.

None the less, this is not the whole story even for the extreme NLS1 as the shape of the soft excess is much broader than predicted by a bare disc spectrum, indicating some Compton upscattering by warm, optically thick material. We associate this with the disc itself, so it must ultimately be powered by mass accretion. We build an energetically self-consistent model assuming that the emission thermalizes to a (colour temperature corrected) blackbody only at large radii. At smaller radii the gravitational energy is split between powering optically thick Comptonized disc emission (forming the soft X-ray excess) and an optically thin corona above the disc (forming the tail to higher energies). We show examples of this model fit to the extreme NLS1 RE J1034+396, and to the much lower Eddington fraction broad-line Seyfert 1 PG 1048+231. We use these to guide our fits and interpretations of three template spectra made from co-adding multiple sources to track out a sequence of active galactic nucleus (AGN) spectra as a function of $L/L_{\rm Edd}$.

Both the individual objects and template spectra show the surprising result that the Compton upscattered soft X-ray excess decreases in importance with increasing $L/L_{\rm Edd}$. The strongest soft excesses are associated with low mass accretion rate AGN rather than being tied to some change in disc structure around Eddington. We argue that this suggests a true break in accretion flow properties between stellar and supermassive black holes.

The new model is publicly available within the XSPEC spectral fitting package.

Key words: accretion, accretion discs – black hole physics – galaxies: active.

1 INTRODUCTION

High mass accretion rate active galactic nucleus (AGN) ubiquitously shows a 'soft X-ray excess', where the X-ray data below 1 keV lie above the low energy extrapolation of the best-fitting 2–10 keV power law. The origin of this feature is currently the subject of active research, but plainly it is generally too hot to be the standard optically thick disc. Relativistic, optically thick, geometrically thin accretion disc models (Novikov & Thorne 1973; Shakura & Sunyaev 1973) give a maximum effective temperature of the accreting material of $kT \sim 10(\dot{m}/M_8)^{1/4}$ eV, where $\dot{m}$ is mass accretion rate in units of Eddington (so that $\dot{m} = \dot{M}/\dot{M}_{\rm Edd} = L/L_{\rm Edd}$), and $M_8 = M/10^8\,{\rm M}_\odot$. Thus the disc spectrum of a typical quasar with a $10^8\,{\rm M}_\odot$ black hole accreting at $L/L_{\rm Edd} = 0.2$ peaks in the extreme ultraviolet (EUV) range, at $\sim 2.7k_{\rm B}T \sim 20$ eV, and the Wein shape above this energy means that it makes very little contribution to the soft X-ray flux above 0.3 keV (e.g. Laor et al. 1997).

This assumes that the emission is able to thermalize completely. This is unlikely to always be true as AGN discs can be dominated by electron scattering rather than absorption in regions where the temperature is well above the hydrogen ionization energy of 13.7 eV

⋆E-mail: chris.done@durham.ac.uk

or 10^5 K (e.g. Ross, Fabian & Mineshige 1992). Such high disc temperatures are found only for a combination of lower black hole mass and higher $L/L_{\rm Edd}$, so this is an effect which will be preferentially important in the narrow-line Seyfert 1 (NLS1) subclass of AGN, objects which often have particularly prominent soft X-ray excesses (see e.g. Boller, Brandt & Fink 1996).

While this could increase the extent of the disc emission in the soft X-ray regime, its predicted shape is a Wien tail which drops much more sharply with energy than the observed, more gradual decline of the soft X-ray excess (Bechtold et al. 1987; Laor et al. 1997). Instead, the observed spectral shape can be fit by Compton upscattering. Clearly there is at least one Compton upscattering region required to produce the power law seen beyond 2 keV, above which the soft excess is measured. The high energy extent of this power law means that the electrons are hot ($kT_{\rm e} \sim 100$ keV), and have low optical depth, $\tau \sim 1$ (e.g. Zdziarski et al. 1995; Zdziarski, Johnson & Magdziarz 1996). To additionally make the very different shape of the soft excess from Compton upscattering requires that there is another electron population, one which has much lower temperature and higher optical depth (Bechtold et al. 1987; Czerny & Elvis 1987).

Physically, this component could arise in a transition region between the disc and hot corona, either separated radially (Magdziarz et al. 1998) or vertically (Janiuk, Czerny & Madejski 2001). However, a key problem with this interpretation is that the temperature associated with the Comptonization region is observed to remain remarkably constant at ∼0.2 keV in all high mass accretion rate AGN (Czerny et al. 2003; Gierliński & Done 2004). A Comptonization region with optical depth τ, heated by power $\ell_{\rm h}$ and cooled by illumination of soft seed photon power $\ell_{\rm s}$ has temperature which is determined by both $\ell_{\rm h}/\ell_{\rm s}$ *and* τ (see e.g. Done 2010, section 1.3.2). A fairly constant temperature then requires that these two parameters are correlated, which seems fine-tuned. Indeed, in black hole binaries (BHBs) where the coronal spectra sometimes require two Comptonization components, the temperature of the optically thicker/lower temperature component clearly varies (see e.g. fig. 4 of Kubota & Done 2004).

An alternative scenario is where the low temperature, optically thick Comptonization is instead the intrinsic spectrum of the disc itself. Substantial changes in disc structure from that predicted by a Shakura–Sunyaev disc might be expected as the accretion rate approaches the Eddington limit. This is especially attractive for some extreme NLS1 objects, where the luminosity is around Eddington and where the soft excess is observed to be less variable than the 2–10 keV power law (Jin et al. 2009; Middleton et al. 2009). Comptonization of the disc emission could occur in the disc itself if there is enhanced dissipation in the upper layers of the disc, over and above that expected from the Shakura–Sunyaev prescription (e.g. Davis et al. 2005). While this could be produced by the magnetorotational instability (MRI: the physical mechanism transporting angular momentum; Balbus & Hawley 1991) there is currently no straightforward way to parametrize the effects of this with increasing mass accretion rate (e.g. Blaes et al. 2011). However, it is clear that as the mass accretion rate approaches Eddington there are several other effects which could act to distort the disc spectrum, such as if the MRI drives large-scale turbulence (Socrates, Davis & Blaes 2004) or if radially advected radiation associated with a slim disc (Abramowicz et al. 1988) can be released in the plunging region (Sądowski 2009).

Thus there are some possibilities to produce the soft excess from the disc itself (as opposed to a separate corona), where the inner disc emission emerges as Compton upscattered flux rather than as a colour temperature corrected blackbody. If so, then a key aspect of the resulting spectrum is that it is powered by the mass accreting through the disc, so the total energy is set by the black hole mass, spin and mass accretion rate through the outer disc. The former can now be constrained via the mass scaling relationships (e.g. Kaspi et al. 2000). The level of optical/UV flux from the disc then directly determines the mass accreting through the outer disc (e.g. Davis & Laor 2011). Here we build a model incorporating these ideas, and demonstrate that at least part of the soft excess seen in the lowest mass, highest mass accretion rate AGN must be intrinsic emission from the disc itself.

2 DISC MODELS

We build a standard blackbody disc model, for a mass accretion rate $\dot{M}$ g s^{-1} on to a black hole of mass M and spin a_* using the effective temperature as a function of radius as derived from the Novikov–Thorne relativistic disc emissivity. We integrate the fluxes from each annulus in the disc over all radii from $r_{\rm out}$ down to the last stable orbit and assume that the emission is isotropic. The black dashed line in Fig. 1(a) shows the spectrum produced by this for a Schwarzschild black hole of mass $M = 10^6\,{\rm M}_\odot$, accreting at the Eddington limit, with $r_{\rm out} = 10^5 R_{\rm g}$, where $R_{\rm g} = GM/c^2$. This has a peak temperature of 4×10^5 K, which is too cool to extend to soft X-ray energies. Extreme spin and/or substantial Compton upscattering is required in order to make significant soft X-ray emission from a disc where the emission thermalizes to the local blackbody temperature (e.g. Laor et al. 1997).

However, disc spectra are more complex than a simple sum of blackbodies at the effective temperature, $B_\nu(T)$, as the true absorption opacity, $\kappa_{\rm abs}(\nu)$, can be substantially smaller than the electron scattering opacity, $\kappa_{\rm T}$, leading to a modified blackbody spectrum, $I_\nu(T) \sim \sqrt{\kappa_{\rm abs}/\kappa_{\rm tot}}B_\nu(T)$, where $\kappa_{\rm tot} = \kappa_{\rm abs} + \kappa_{\rm T}$ (Shakura & Sunyaev 1973; Czerny & Elvis 1987).

Absorption opacity, $\kappa_{\rm abs}$, depends on temperature, density and frequency, whereas the electron scattering opacity is constant. Thus $\kappa_{\rm abs}/\kappa_{\rm es}$ and hence the detailed spectrum is sensitive to the vertical structure of the disc. For a given density, the absorption opacity is lower at higher temperature, so the effective photosphere where $\tau_{\rm eff} \approx \tau_{\rm T}\sqrt{\kappa_{\rm abs}(\nu)/\kappa_{\rm T}} = 1$ is at a greater depth in the disc. The temperature increases with depth, so the difference between this temperature and the surface temperature increases, giving an increased colour temperature correction. However, the increased depth of formation also increases the number of scatterings before escape in the lower temperature material between the photosphere and the surface, increasing Compton downscattering which lowers the colour temperature correction. Davis, Done & Blaes (2006) show that these two competing effects lead to the effective saturation of the colour temperature correction to a value

$$f_{\rm col} \sim (72/T_{\rm keV})^{1/9} \quad (1)$$

(their equation A13). They derived this in the context of BHB discs, where the typical effective temperature of ∼1 keV gives a predicted $f_{\rm col} \sim 1.6$ which has very little dependence on mass accretion rate as $T \propto (L/L_{\rm Edd})^{1/4}$ so $f_{\rm col} \propto (L/L_{\rm Edd})^{1/36}$. This is consistent with the observed $L \propto T^4$ behaviour (which implies constant colour temperature correction as well as constant inner radius) seen in BHB-disc-dominated spectra over a wide range in $L/L_{\rm Edd}$ (Shimura & Takahara 1995; Kubota, Makishima & Ebisawa 2001; Gierliński & Done 2004).

While equation (1) was derived for BHB discs, its assumptions should also hold in AGN discs. The first and most important

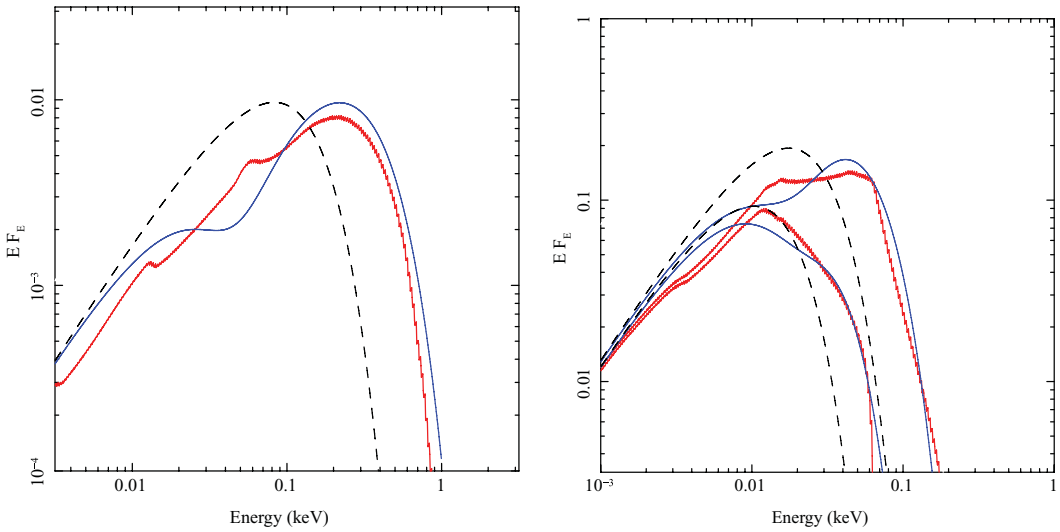

Figure 1. Accretion disc spectra for a Schwarzschild black hole. The black dashed line is the spectrum from a standard Shakura–Sunyaev disc assuming that the energy thermalizes completely, while the blue solid line has a single colour temperature correction applied to all radii with $T > T_{\rm scatt}$ and the red line is the disc spectrum calculated from the full radiative transfer code; (a) has 10^6 M$_\odot$ and $L/L_{\rm Edd} = 1$ with $f_{\rm col} = 2.34$ for $T > T_{\rm scatt} = 10^5$ K, while (b) has 10^8 M$_\odot$, $L/L_{\rm Edd} = 0.2$ with $f_{\rm col} = 2$ together with 2×10^8 M$_\odot$ and $L/L_{\rm Edd} = 0.05$ and $f_{\rm col} = 1.8$, both with $T_{\rm scatt} = 4 \times 10^4$ K.

assumption is that electron scattering dominates, i.e. that $\kappa_{\rm abs} \ll \kappa_{\rm es}$. Typically, $\kappa_{\rm abs} \propto nT^{-\beta}$, where n is the density, and $\beta = 3.5$ for free–free absorption. However, bound–free absorption edges are typically more important. Each individual edge gives $\beta = 2.7$–3 but added together the effect from all ionization states of all elements coincidentally gives $\beta \sim 3.5$. BHB discs are at much higher temperature than AGN discs as $T \propto M^{-1/4}$, typically with $T \sim 10^7$ K where the absorption opacity is dominated by the metal edges. These have much lower abundance than hydrogen and helium, which typically dominate the bound–free opacity at AGN disc temperatures of $T \sim 10^5$ K. None the less, this increase in opacity with decreasing temperature is more than offset by the lower density of AGN discs, as $n \propto M^{-1}$ so $\kappa_{\rm abs} \propto M^{-1}[M^{-1/4}]^{-3.5} \propto M^{-1/8}$. Thus for the same luminosity in terms of Eddington, $L/L_{\rm Edd}$, scattering is more important in an AGN disc than in a BHB disc.

The other assumptions on the temperature and density structure of the outer layers of the radiation-pressure-dominated disc should be equally applicable to AGN and BHB discs. The only other caveat is that there is no significant additional dissipation of energy above the effective photosphere, i.e. we must be able to treat it as an atmosphere, otherwise the colour temperature correction increases further (Done & Davis 2008). Hence we should be able to apply equation (1) to AGN discs also, and we can test this by comparison with full disc radiative transfer models. Pioneering calculations by Ross et al. (1992) showed $f_{\rm col} \sim 2.4$ for a 10^6 M$_\odot$ Schwarzschild black hole accreting at $L/L_{\rm Edd} = 0.33$. These disc parameters predict a peak disc temperature of 3×10^5 K, so equation (1) gives $f_{\rm col} = 2.4$, in excellent agreement with Ross et al. (1992).

We use the Hubeny et al. (2001) models, recalculated as in Davis & Hubeny (2006), to independently test equation (1). This uses the Novikov–Thorne emissivity, but includes full radiative transfer through the vertical structure of the disc at each radius, taking into account both Compton scattering and full metal opacities (bound–free). Unlike our model, the resulting radiation is then propagated to the observer with full general relativistic corrections, but these make little difference for a low spin, especially as the gravitational redshift more or less cancels the Doppler blueshift at our chosen inclination of 60° for a Schwarzschild black hole (Zhang, Cui & Chen 1997).

The red line in Fig. 1(a) shows this full disc spectrum calculated for a 10^6 M$_\odot$ Schwarzschild black hole accreting at $L/L_{\rm Edd} = 1$. The peak effective disc temperature of 4×10^5 K gives $f_{\rm col} = 2.34$ from equation (1) for the innermost radii. At larger radii the temperature is lower, so according to equation (1) the colour temperature correction should increase. However, this assumes that electron scattering completely dominates the opacity. This is certainly not true for $T < 10^4$ K, when H is neutral so there are few free electrons, so $f_{\rm col} = 1$ at this point. The blue line in Fig. 1(a) shows a simple colour temperature corrected blackbody disc with $f_{\rm col} = 2.34$ on all annuli with temperature $T > T_{\rm scatt} = 10^5$ K (a conservative point at which electron scattering should completely dominate the opacity as being well beyond the ionization energies of H and He), and $f_{\rm col} = 1$ for temperatures below this. This matches fairly well to the full disc spectrum around the peak, though the abrupt jump in colour temperature from 2.34 to 1 at $T = 10^5$ K gives a sharp change in slope in the EUV spectrum while the full spectrum calculation (red line) is much smoother, showing that the colour temperature correction decreases more gradually with temperature. There is also some residual $f_{\rm col} > 1$ in the optical above the Balmer edge, as shown by the slightly lower normalization of the full disc spectrum in this bandpass, though this effect is much smaller than the potential change in normalization arising from different inclination angles (see e.g. Hubeny et al. 2001).

The value of the colour temperature correction in the general case where electron scattering is not overwhelmingly dominant is not possible to estimate analytically, as it depends on the details of the vertical structure. We estimate this instead from full radiative transfer disc spectral calculations. The red lines in Fig. 1(b) show the results of this for Schwarzschild black holes with mass 10^8 M$_\odot$ at $L/L_{\rm Edd} = 0.2$ (upper lines) compared to 2×10^8 M$_\odot$ at $L/L_{\rm Edd} = 0.05$. The total luminosity $L = \eta \dot{M} c^2$ is simply set by the total mass accretion rate $\dot{M} \propto ML/L_{\rm Edd}$ and black hole efficiency, η, so is a factor of 2 higher for the spectrum with 10^8 M$_\odot$ at $L/L_{\rm Edd} = 0.2$. Conversely, the optical luminosity is set by the combination of $M\dot{M}$ (e.g. Davis & Laor 2011) $\propto M^2 L/L_{\rm Edd}$, i.e. is the same

for both models. The full radiative transfer spectra (red solid lines) again have strong edge features, so are not well described by a set of (colour temperature corrected) blackbodies. None the less, these spectra can be roughly modelled with $T_{\rm scatt} = 4 \times 10^4$ K and $f_{\rm col} = 2$ and 1.8 for (M, $L/L_{\rm Edd}$) of ($10^8\,{\rm M}_\odot$, 0.2) and ($2 \times 10^8\,{\rm M}_\odot$, 0.05), respectively (blue lines). Complete thermalization ($f_{\rm col} = 1$) is shown as the black dashed line. This is not very different to the full spectrum for $M = 2 \times 10^8\,{\rm M}_\odot$, $L/L_{\rm Edd} = 0.05$ as the highest temperature in the (blackbody) disc is only 5.4×10^4 K. Thus He is mainly neutral, reducing the number density of free electrons, and the absorption opacity is starting to reach its peak around the ionization of hydrogen (see e.g. Hure et al. 1994). Thus electron scattering is not overwhelmingly dominant, so equation (1) overestimates $f_{\rm col}$ at 2.9.

Davis & Laor (2011) show that electron scattering is even less important for the case of a Schwarzschild black hole at $M = 10^8\,{\rm M}_\odot$, $L/L_{\rm Edd} = 0.027$ (i.e. $\dot{M} = 0.1\,{\rm M}_\odot\ {\rm yr}^{-1}$), as the blackbody disc is a fairly good approximation to the full radiative transfer disc spectrum, i.e. the $f_{\rm col} \rightarrow 1$ as the disc temperature drops below 3×10^4 K, where H starts to become neutral so the associated absorption edge opacity is large.

We can approximate the change in colour temperature correction as

$$f_{\rm col} \sim (T_{\rm max}/3 \times 10^4)^{0.82} \qquad (2)$$

over the critical temperature range of $3 \times 10^4 < T_{\rm max} < 10^5$ K. This changes linearly with $T_{\rm max}$ from unity to 2.7 (the value of $f_{\rm col}$ from equation 1 for $T_{\rm max} = 10^5$ K). Electron scattering should dominate above 10^5 K, so $f_{\rm col}$ is then given by equation (1), and decreases slowly with $T_{\rm max}$.

Thus the observed maximum disc temperature increases as $T_{\rm max,obs} = T_{\rm max} f_{\rm col}(T_{\rm max}) \propto T_{\rm max}^{1.82} \propto [(L/L_{\rm Edd})/M]^{0.46}$ in the range $3 \times 10^4 < T_{\rm max} < 10^5$ K. This is much faster than the $[(L/L_{\rm Edd})/M]^{0.25}$ dependence predicted from purely blackbody models. Fig. 2 shows how the disc spectrum can be fairly well matched to the full radiative transfer models by combining equations (1) and (2) to calculate $f_{\rm col}$ at each radius in the disc.

In summary, the spectrum of a bare accretion disc can be roughly described by a colour temperature corrected sum of blackbody spectra, where the value of the colour temperature correction factor is approximately unity in the optical part of the spectrum, but is higher above the Lyman break where hydrogen and helium are ionized and electron scattering can dominate. Where scattering is completely saturated, the colour temperature correction is as large as predicted by equation (1), but this only occurs for a disc with intrinsically high temperature, i.e. for high $L/L_{\rm Edd}$ and low black hole mass, i.e. for NLS1s. This colour temperature correction accentuates the expected increase in disc temperature for these objects due to their low mass/high mass accretion rate. This increases the distinction in EUV and hence emission-line properties between objects with low $(L/L_{\rm Edd})/M$ [typically broad-line Seyfert 1 (BLS1) galaxies] and those with high $(L/L_{\rm Edd})/M$ (typical NLS1s).

3 COMPTONIZED DISC EMISSION FOR THE SOFT X-RAY EXCESS

Fig. 3 shows this full radiative transfer AGN spectrum (red line) compared to the X-ray spectrum of the NLS1 RE J1034+394 (black data points) assuming a distance of 188 Mpc as appropriate for its redshift of 0.04. This is one of the most extreme NLS1 systems, with permitted linewidths which are amongst the lowest seen (Grupe et al. 2004). Subtracting the narrow component of Hβ using the [O III] line profile gives a residual which has a full width at half-maximum (FWHM) of $988\,{\rm km\,s^{-1}}$ indicating a black hole mass of $\sim 1.5 \times 10^6\,{\rm M}_\odot$ when combined with the optical luminosity of $\lambda L_{5100} = 1.9 \times 10^{43}\,{\rm erg\,s^{-1}}$ (Jin et al. 2011a, hereafter J11a). The bolometric correction is highly uncertain since the luminosity peaks in the unobservable EUV (Puchnarewicz et al. 2001; Casebeer, Leighly & Baron 2006), but estimates for $L/L_{\rm Edd}$ range from $\sim$1 to 5, so the system parameters are directly comparable to the full radiative

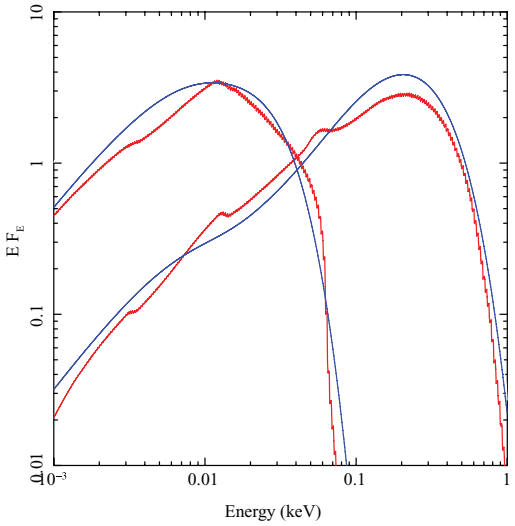

Figure 2. Blue lines show Schwarzschild disc spectra calculated using colour temperature corrected blackbodies with $f_{\rm col}$ given by equations (1) and (2). These compare well to the full radiative transfer disc spectra (red lines), giving smoother spectra than those in Fig. 1 calculated from a single $f_{\rm col}$. The lower temperature spectra are for $M = 2 \times 10^8\,{\rm M}_\odot$ with $L/L_{\rm Edd} = 0.05$, while the higher temperature spectra are for $M = 10^6\,{\rm M}_\odot$ with $L/L_{\rm Edd} = 1$.

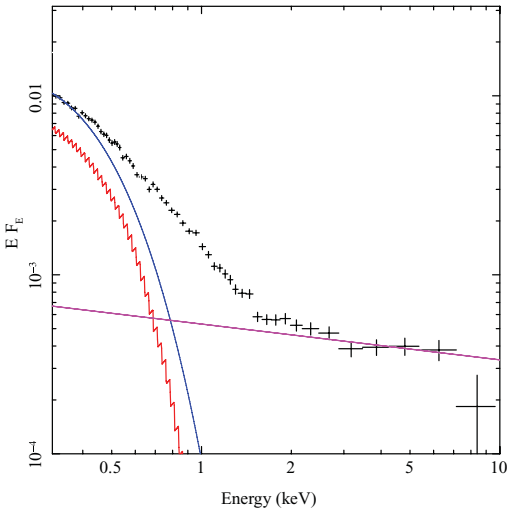

Figure 3. The *XMM–Newton* PN spectrum of RE J1034+396 (black points) compared to the full radiative transfer disc spectrum for $M = 10^6\,{\rm M}_\odot$, $L/L_{\rm Edd} = 1$ (red), together with the colour temperature corrected blackbody disc spectrum for $M = 10^6\,{\rm M}_\odot$, $L/L_{\rm Edd} = 1.15$ (blue). This can account for most of the 'soft X-ray excess' in this object, though the shape of the predicted disc spectrum is too steep to match the observed data in the 0.5–1 keV energy range even including the best-fitting 2–10 keV power law (magenta line).

transfer disc model. We include the best-fitting 2–10 keV power-law spectrum (magenta line), and Galactic absorption column of 1.47×10^{20} cm^{-2}. Fig. 3 shows that the predicted emission from the disc itself, even without Compton upscattering, will extend into the soft X-ray range for such a low black hole mass/high mass accretion rate. However, it also illustrates that the disc spectrum rolls over too rapidly to explain the 0.6–2 keV emission, so some Compton upscattering is required.

As briefly outlined in the Introduction, the problem is that the soft excess appears to have a remarkably constant temperature, which seems fine-tuned for external Comptonization models. Intrinsic disc Compton scattering gives more scope for a 'thermostat' e.g. enhanced dissipation in the upper layers of the disc over and above that expected from the Shakura–Sunyaev prescription (e.g. Davis et al. 2005). Enhanced dissipation away from the mid-plane is indeed found in self-consistent simulations of the vertical structure produced with the MRI in a radiation-pressure-dominated disc (Blaes et al. 2011). The effective depth of the photosphere then controls both ℓ_h/ℓ_s and τ, such that seeing deeper into the disc means that there is both additional dissipation to heat the electrons but also larger optical depth of electrons. This might result in an energy per electron (i.e. temperature) which is fairly constant due to this physical correlation between the two parameters.

Alternatively (or additionally) the radiation-pressure-dominated MRI appears to drive large-scale turbulence. This bulk motion, with mean velocity $\langle v^2 \rangle$, can Compton upscatter the emerging disc flux, producing the same spectrum as from $3kT \sim 1/3\langle v^2 \rangle$ (Socrates et al. 2004). The apparent fine-tuning of temperature then instead requires a constant typical turbulent velocity which should scale mainly with $\dot{m}$ rather than black hole mass (Socrates et al. 2004). The AGN sample of Gierliński & Done (2004) mostly had high mass accretion rate objects, so the range in $\dot{m}$ is rather small giving a similarly small range in characteristic temperature for the bulk Compton upscattering. We note that this could also explain why this component does not seem to be present in BHB, as their much higher temperature discs means that it would be unaffected by the typical $kT \sim 0.2$ keV of the soft excess component seen in AGN.

Further possibilities include changes in disc structure due to advection of radiation at high mass accretion rates (slim discs; Abramowicz et al. 1988). The disc becomes so optically thick that photons are swept radially along with the flow before they can diffuse outwards. However, the rapid increase in velocity in the plunging region means that the flow can become optically thin at this point, so some of the radiation can escape from within the innermost stable circular orbit (Sądowski 2009).

Whatever the origin, a simple approach to fitting the soft X-ray data is to assume that there is an additional Compton upscattered component e.g. the XSPEC model COMPTT (Titarchuk 1994) as well as the optical/UV emitting disc. However, it is difficult to uniquely determine the parameters of two independent components especially given the lack of data in the EUV region (see e.g. Jin et al. 2009). More fundamentally, the Comptonized emission should also be powered ultimately by the accretion flow, so the two components should be energetically coupled.

Done & Kubota (2006, hereafter DK06) developed a model including this energetic coupling for the strongly Comptonized very high state of Galactic BHBs. Here we develop a version of this model which is much faster (so is more appropriate for fitting multiple spectra), and which explicitly uses the physical parameters as inputs (see Appendix A for a comparison of the two models).

We assume that this Compton upscattering takes place in the disc itself, so the luminosity in this Comptonization component should

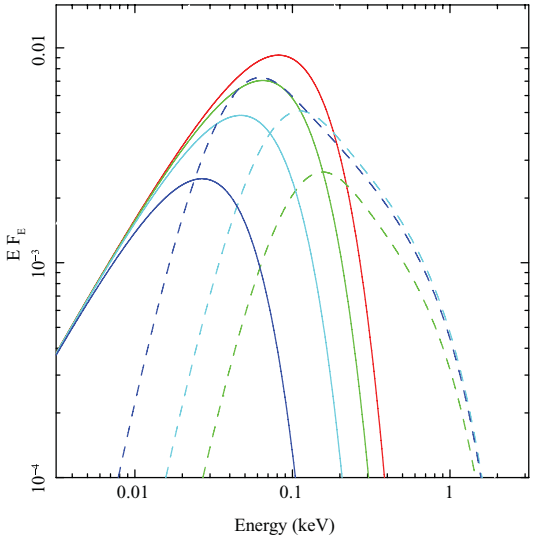

Figure 4. The model spectra for a disc where the accretion flow thermalizes into blackbody emission with $f_{col} = 1$ for radii $r > r_{corona}$ (solid line). Below this radius the energy is dissipated by Compton upscattering of seed photons at the disc temperature at r_{corona} by electron with temperature of 0.22 keV and optical depth of 15 (dotted line). The red, green, cyan and blue models are calculated for $r_{corona} = 6$, 16, 30 and 75, corresponding to 0 (pure disc), 25, 50 and 75 per cent of the total accretion power in the Compton upscattering region.

be the same as that of the disc luminosity at each radius. Thus once the mass and mass accretion rate through the outer disc are set, the total luminosity of the Compton upscattered flux is completely determined by the integral of the emissivity from r_{corona}, the radius at which the emission starts to emerge as Comptonized rather than (colour temperature corrected) blackbody, to r_{isco}, the last stable orbit. We assume that the energy within r_{corona} is emitted as Compton upscattered flux (COMPTT), with seed photons characterized by the (colour temperature corrected) disc temperature at r_{corona}.

We illustrate the dependence of the spectrum on r_{corona} in Fig. 4 for our fiducial system (black hole mass of 10^6 M$_\odot$ at $L/L_{Edd} = 1$ calculated with $f_{col} = 1$). We show results for $r_{corona} = 6$ (i.e. same as the black dashed line in Fig. 1a), 16, 30 and 75, corresponding to 0, 25, 50 and 75 per cent of the total accretion power dissipated in the corona, respectively (red, green, cyan and blue lines). The solid lines show the emission from the outer disc, while the dotted lines show the increasing power in the soft Comptonization component, all of which have $kT_e = 0.22$ keV and $\tau = 15$. For these parameters the Comptonized spectrum is steep, so it peaks at the seed photon temperature which decreases with increasing r_{corona}, as is also seen in the lower maximum temperature emission from the blackbody disc emission. The optical/near-UV region is dominated by the outer disc emission, so is the same for all the models considered here.

As discussed in Appendix A, our assumption of the seed photon energy as being set by the disc temperature at r_{corona} may not be accurate for very large r_{corona}. Steep Comptonized spectra peak at ($\sim$4 $\times$) their seed photon temperature (see Fig. 4), so the spectrum can peak at energies lower than that of the thermalized disc for $r_{corona} > 75$ which is probably unphysical. Seed photons generated internally in the Comptonization region probably are more important, and these would have higher temperature. We stress that the derived parameters should be used with caution where r_{corona} is large and the Comptonization is steep.

4 MODELLING THE SED OF A NLS1: RE J0134+396

While this gives a model for the soft excess, there is also higher energy emission above 2 keV (see Fig. 3). The energy to power this must also ultimately be derived from mass accretion, so we assume that some fraction, $f_{\rm pl}$, of the energy dissipated from $r_{\rm corona}$ to $r_{\rm isco}$ powers this high-energy Comptonization component. We model this using NTHCOMP code in XSPEC (Zdziarski et al. 1996), again setting the seed photon temperature equal to that of the (colour temperature corrected) blackbody from the disc at $r_{\rm corona}$.

Thus the full model contains three distinct spectral components, but these are all powered by the energy released by a single accretion flow of constant mass accretion rate, $\dot{M}$, on to the black hole of mass M. The outer disc emission is the colour temperature corrected blackbody emission from $r_{\rm out}$ to $r_{\rm corona}$, where $f_{\rm col}$ is only applied on annuli with temperature $T > T_{\rm scatt}$. A fraction $f_{\rm pl}$ of the remaining energy emitted as the mass accretes from $r_{\rm corona}$ to $r_{\rm isco}$ is emitted as the high-energy (above 2 keV) Comptonization, characterized by a power law of photon index Γ and electron temperature fixed at 100 keV, while the remaining fraction $(1 - f_{\rm pl})$ is emitted as low temperature, optically thick Comptonization of the disc emission, parametrized by $kT_{\rm e}$ and τ. Fig. 5 shows a schematic of these three regions, together with their spectra. We call this full model OPTXAGN, and have made it publicly available as a local model for the XSPEC spectral fitting package (Arnaud 1996). We also include an additional model, OPTXAGNF, incorporating the approximate $f_{\rm col}(T_{\rm max})$ relationship of equations (1) and (2). In both versions, the overall normalization is set explicitly by the model parameters, so the normalization must be frozen to unity. Inclination angle could change this by a factor of ∼2 (see e.g. Hubeny et al. 2001), but this is beyond the scope of the model.

We fit the full model to the broad-band spectral energy distribution (SED) assembled by J11a, including absorption by two gas columns, one fixed at the Galactic value along the line of sight and the other allowed to be free to model intrinsic absorption associated with the host galaxy and/or nucleus. Each of these two gas columns is assumed to have a standard gas to dust ratio, $E(B-V) = 1.7(N_{\rm H}/10^{22}\,{\rm cm}^{-2})$, producing optical reddening which is tied to the X-ray absorption (see J11a).

We allow a range of black hole mass, corresponding to the FWHM of the intermediate and broad components of Hβ (918 and 4400 km s^{-1} giving $1.2 \times 10^6 < M < 2.9 \times 10^7\,{\rm M}_\odot$, respectively), Fig. 6 shows the best-fitting, absorption corrected, model together with the data for REJ1034+396 assuming $f_{\rm col} = 1$ (black, as assumed in J11a) and for $f_{\rm col} = 2.4$, $T_{\rm scatt} = 10^5$ K (magenta, as in Fig. 1). We show the full optical/UV SED points from J11a but only include the highest frequency UV point in the fit (*XMM–Newton* OM UVW2) as the continuum emission has a very different spectrum to that expected from a disc even in the UV (Casebeer et al. 2006). This is probably due to there being an additional continuum component, most probably starlight contamination from the host galaxy (Sani et al. 2010).

Fig. 6 shows that the models differ in the unobservable EUV regime, but both are consistent with the UV flux limits for the disc emission, and both fit the soft X-ray data well, with best-fitting parameters given in Table 1. The spectral slope of the soft X-ray excess sets the Comptonization parameters, $kT_{\rm e}$ and τ, and extends down to the seed photon energy, set by the inner disc temperature at $r_{\rm corona}$. This is where the luminosity peaks for a steep soft X-ray excess, and so the substantially higher seed photon

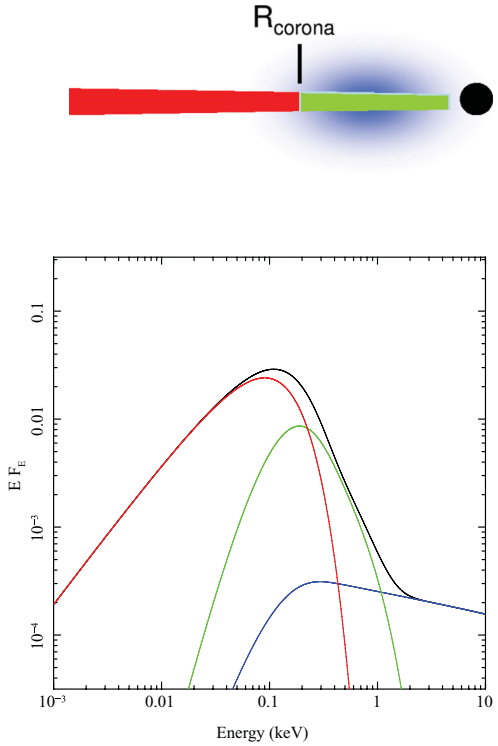

Figure 5. A schematic of the model geometry and resultant spectra, with outer disc (red) which emits as a (colour temperature corrected) blackbody, and an inner disc (green) where the emission is instead Compton upscattered (perhaps by bulk turbulent motion in the disc, or by there being more dissipation in the effective photosphere than assumed in the standard Shakura–Sunyaev vertical dissipation profile). Some fraction of the energy is also Compton upscattered in a corona (blue) to produce the power-law tail to high energies.

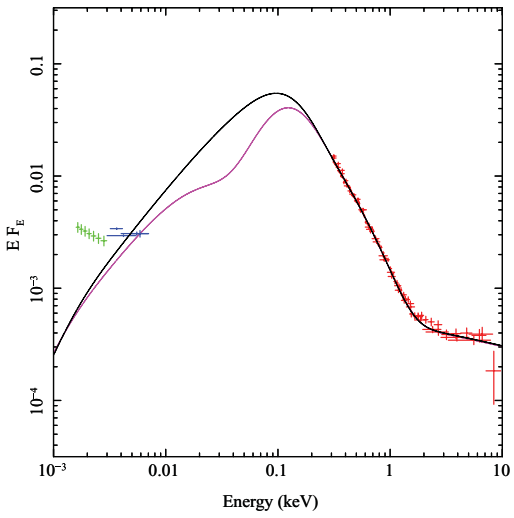

Figure 6. The *XMM–Newton* X-ray (red) and Optical Monitor (blue) data from RE J1034+396, together with (non-simultaneous) Sloan Digital Sky Survey optical continuum points (green) from J11a. These are shown (absorption corrected) with the best-fitting models with $f_{\rm col} = 1.0$ (black) and 2.6 (magenta). The fit only includes the highest frequency UV (UVW2) point as *Hubble Space Telescope* data show that the disc only dominates in the far-UV. The models differ mainly in the unobservable EUV, but $L/L_{\rm Edd}$ differs only by a factor of 2 and all other model parameters are similar (see Table 1).

Table 1. Details of fits to the NLS1 RE 1034+396 using the intrinsic Comptonization model for the soft excess. The first line has $f_{\rm col} = 1.0$ while the second is for $f_{\rm col} = 2.4$.

$N_{\rm H}$ (10^{20} cm^{-2})	$f_{\rm col}$	M (10^6 M$_\odot$)	$L/L_{\rm Edd}$	$r_{\rm corona}$ ($R_{\rm g}$)	$kT_{\rm e}$ (keV)	τ	Γ	$f_{\rm pl}$	χ^2/ν
1.7 ± 0.7	1.0	$1.2^{+0.1}$	$5.0^{+0.7}_{-0.6}$	31^{+14}_{-9}	0.23 ± 0.03	11 ± 1	2.2	0.05 ± 0.02	631/563
1.6 ± 0.6	2.4	$1.9^{+0.8}_{-0.1}$	$2.4^{+0.3}_{-0.6}$	100^{+*}_{-60}	0.23 ± 0.03	11 ± 1	2.2	0.05 ± 0.02	630/563

*indicates that the parameter is pegged at the upper/lower limit.

temperature arising from $f_{\rm col} = 2.6$ compared to $f_{\rm col} = 1$ results in a substantially lower total luminosity. The accretion efficiency, η, is fixed by black hole spin (assumed to be 0), so the total luminosity $L = \eta \dot{M} c^2$ sets the total mass accretion rate. Conversely, the optical luminosity is set by the combination of $M\dot{M}$ (e.g. Davis & Laor 2011), so for a higher $\dot{M}$ to fit the same optical/UV flux points requires a lower black hole mass. Thus the model with $f_{\rm col} = 1$ has both a higher $\dot{M}$ and lower M (and hence much higher $L/L_{\rm Edd}$) than the corresponding model with $f_{\rm col} = 2.4$, but none of the other parameters changes significantly.

5 MODELLING THE SED OF A BLS1: PG 1048+342

While the disc almost certainly contributes to the soft excess in low mass, high mass accretion rate AGN such as RE J1034+396, the same should not be true for the higher mass, lower mass accretion rate broad-line AGN as the disc temperature is lower. This temperature is too low for electron scattering to ever dominate so there is no substantial colour temperature correction (see Fig. 1b), pulling the intrinsic disc emission even further away from the soft X-ray region. None the less, these objects still show a soft X-ray excess. We illustrate this using the SED of PG 1048+213, which has a black hole mass of $\sim 2 \times 10^8$ M$_\odot$, and $L/L_{\rm Edd} \sim 0.1$ (J11a). Fig. 7(a) shows the deconvolved spectrum for $f_{\rm col} = 1.0$, and it is clear that not only is the disc intrinsically cool, but that the fit requires a very

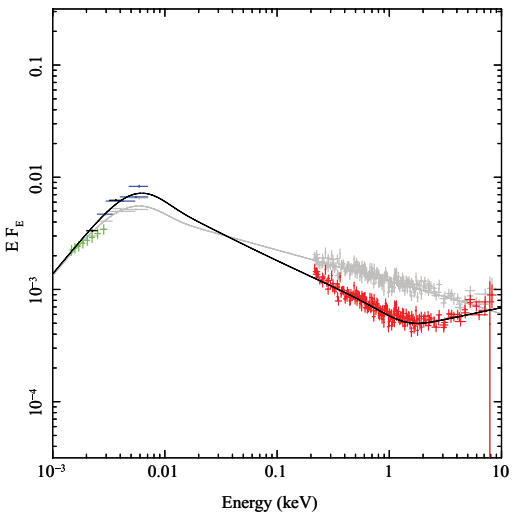

Figure 7. As for Fig. 6 but for the BLS1 PG 1048+213. The best-fitting model with $f_{\rm col} = 1.0$ (black) is shown, but this is identical to one with $f_{\rm col} = 2$ as the maximum disc temperature at $r > r_{\rm corona}$ is always less than $T_{\rm scatt} = 4 \times 10^4$ K. The grey line and data show the different resulting SED derived from assuming that there is complex absorption producing the dip in the X-ray spectrum. None the less, both models give a similarly large non-disc component.

large $r_{\rm corona}$ in order to produce the observed X-ray emission (both soft excess and higher energy power law), so that only the coolest outer disc contributes to the thermalized emission.

While the model fits the data well, it illustrates some of the more puzzling issues associated with the soft X-ray excess. While turbulent motions may well give rise to bulk Comptonization, the mass accretion rate here is approximately 10 times lower in terms of Eddington fraction than for RE J1034+396, yet the electron temperatures for the soft Comptonization are very similar. Other issues are that the 2–10 keV power law is quite flat with $\Gamma = 1.7$, i.e. rising in νf_ν. This looks much more similar to the low/hard state in BHB systems, yet these are seen only at much lower Eddington fractions ($L/L_{\rm Edd} \lesssim 0.02$) except in the non-equilibrium states triggered by the dramatic outbursts in Galactic binary systems (Nowak 1995; Maccarone 2003; Gladstone, Done & Gierliński 2007; Yu & Yan 2009). The clear disc component in the optical/UV SED and its dominance over the level of X-ray emission makes this appear more similar to the high/soft state in Galactic BHBs, but these have $\Gamma = 2$–2.2 (see e.g. the review by Done, Gierliński & Kubota 2007, hereafter DGK07).

These issues have motivated alternative ways to model the soft X-ray excess, as a distortion from atomic processes. There is a strong jump in opacity at 0.7 keV from partially ionized material, where O VII/O VIII and the Fe M shell unresolved transition array (UTA) combine to produce much more absorption above this energy than below. This could produce an *apparent* (rather than intrinsic) soft excess in two very different geometries, either by reflection from optically thick material out of the line of sight (Fabian et al. 2002), or through absorption by optically thin material in the line of sight (Gierliński & Done 2004; Chevallier et al. 2006). However, both these geometries would show characteristic sharp atomic features (lines and edges). These can be smeared by strong relativistic effects in the reflection model, but the parameters required are quite extreme (the disc has to extend down to the last stable orbit of a high spin black hole, with reflection emissivity which is highly concentrated to the innermost regions; Crummy et al. 2006). In absorption, the line-of-sight velocity shear required to smear out the atomic features is probably unrealistically large (Gierliński & Done 2004; Schurch & Done 2007). However, the absorption model may be substantially more complex as the high columns inferred mean that resonance line scattering should be important (Sim et al. 2010), and the absorption can be clumpy so that it covers only part of the source, diluting the expected line absorption signature (Miller et al. 2007; Turner et al. 2007; Miller, Turner & Reeves 2009; Risaliti et al. 2011).

Given the limited signal-to-noise ratio of our X-ray data, we model the effects of absorption and/or reflection using a simple neutral partial covering model. This assumes that some fraction, $C_{\rm f}$ of the X-ray source is covered by a neutral column of $N_{\rm H}$, while the rest is unobscured. Since this model can match the whole X-ray spectrum with a single power law, there is no need for a separate soft excess component. Hence we assume that all the gravitational energy released from inside $r_{\rm corona}$ goes into powering the high-energy tail. The grey data and model line in Fig. 7 show the resulting

Table 2. Details of fits to the BLS1 PG 1048+213. The first fit is for the intrinsic Comptonization model for the soft excess, the second is for an atomic absorption (partial covering) origin for this feature. While these are both calculated for $f_{\rm col} = 1.0$, models with $f_{\rm col} = 2$ give identical fits as the disc temperature for $r > r_{\rm corona}$ never rises above $T_{\rm scatt} = 4 \times 10^4$ K.

$N_{\rm H}$ (10^{20} cm^{-1})	$f_{\rm col}$	$L/L_{\rm Edd}$	$r_{\rm corona}$ ($R_{\rm g}$)	$kT_{\rm e}$ (keV) $N_{\rm H}$	τ $C_{\rm f}$	Γ	$f_{\rm pl}$	χ^2/ν
1.9 ± 0.5	1.0	0.17 ± 0.01	100_{-4}	0.25 ± 0.05	15 ± 1.5	1.80 ± 0.08	0.25 ± 0.02	832/596
0^{+1}	1.0	0.15 ± 0.01	77 ± 9	17 ± 6	0.51 ± 0.03	2.27 ± 0.02	1.0	884/597

inferred SED. While this is somewhat different, the fraction of luminosity in the EUV/X-ray region is similarly high, so $r_{\rm corona}$ is still required to be large in order to power this emission. The inferred luminosity of the Comptonized spectrum after accounting for distortion by complex absorption still contains three times more power than that which thermalizes. If this is powered by material that accretes through the outer thin disc then this requires all the gravitational energy from within $\sim 75 R_{\rm g}$. Unless the hard X-rays are powered by a separate coronal flow, the inescapable conclusion is that the accretion energy cannot thermalize in a thin disc structure down to the last stable orbit. Such a geometry is strongly reminiscent of the truncated disc models for the low/hard state in stellar mass BHB systems, yet the Eddington fraction of ~ 0.15 is relatively high for this state (see e.g. the review by DGK07).

Both models in Table 2 have large $r_{\rm corona}$ and a steep Comptonization spectrum. This means that the full SED peaks at (~ 4 $\times$) seed photon temperature for Comptonization, set by the disc temperature at $r_{\rm corona}$. This probably underestimates the seed photon temperature, as discussed in Section 3, so the (unobservable) EUV part of the spectrum could have somewhat different shape (see Appendix A).

6 MODELLING THE MEAN OPTICAL TO X-RAY SED OF AGN

Having discussed the different issues in fitting a single NLS1 and BLS1 spectrum, we now use the mean spectra as compiled by J11a and Jin et al. (2011b, hereafter J11b) from stacking the derived spectral models from fitting their sample of 51 objects into three subgroups. Of the various possible parameters to group by (e.g. FWHM of Hβ, black hole mass etc.) $L/L_{\rm Edd}$ gave the minimum dispersion, so is the most likely to represent the principle underlying physical parameter which determines the spectral shape (J11b). We refer to these spectra as M1, M2 and M3 for $L/L_{\rm Edd}$ of 0.05, 0.2 and 2.1, respectively.

These three spectra have an associated mean black hole mass which is anticorrelated with $L/L_{\rm Edd}$. It is likely that this is primarily a selection effect. The optical luminosity of the accretion flow is $\propto (M\dot{M})^{2/3}$ (e.g. Davis & Laor 2011) $\propto [M^2(L/L_{\rm Edd})]^{2/3}$. This has to be large enough to be detected above the bulge luminosity of the host galaxy $L_{\rm host} \propto M_{\rm host} \propto M$ (Magorrian et al. 1998). This sets a lower limit on $M(L/L_{\rm Edd})^2$ for the AGN to be detectable. Thus low-mass black holes can only be detected against their (low-mass) host galaxy at high Eddington fractions, while high-mass black holes (hosted by more massive galaxies) can be detected at much lower Eddington fractions. These high-mass black holes would be even more obvious at high Eddington fractions, but such objects are very rare in the local Universe, first as high-mass black holes are much less numerous than low mass ones, and secondly as their large host galaxies form in the most overdense regions, where activity (both star formation and accretion flows on to the nucleus) peaks at redshift ~ 2 then declines as the gas supply runs out. Thus the highest mass black holes in the local Universe typically have low mass accretion rates (downsizing, see e.g. Fanidakis et al. 2011).

We show these mean spectra in Fig. 8, where the overall normalization is arbitrary but is fixed to the same value for all three spectra. The lowest $L/L_{\rm Edd}$ spectrum (M1: blue) has disc to hard X-ray ratio which is typical of Seyferts in the local Universe (Koratkar & Blaes

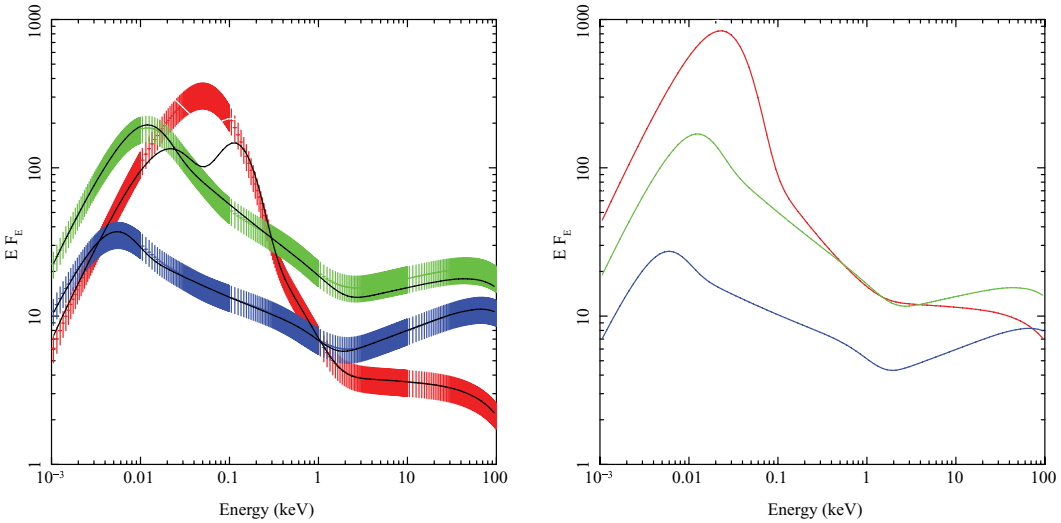

Figure 8. (a) The three mean spectra from J11b, derived using $f_{\rm col} = 1$, but we show the fit (excluding the unobservable 0.01–0.3 keV region) with $f_{\rm col} = 2.5$ for the lowest mass/highest mass accretion rate spectrum, where the disc temperature exceeds $T_{\rm scatt} = 10^5$ K. M1 (blue) has $L/L_{\rm Edd} = 0.058$ and black hole mass of 1.4×10^8 M$_\odot$. M2 (green) has $L/L_{\rm Edd} = 0.23$ and black hole mass of 1.1×10^8 M$_\odot$. M3 (red) has $L/L_{\rm Edd} = 0.77$ and black hole mass of 2.6×10^7 M$_\odot$. (b) It shows the spectral evolution with $L/L_{\rm Edd}$ alone by redoing each model for a single black hole mass of 10^8 M$_\odot$ (and $f_{\rm col} = 1$).

Table 3. Details of fits to the three mean spectra in J11b.

Spectrum	$L/L_{\rm Edd}$	$M\,({\rm M}_\odot)$	$f_{\rm col}$	$r_{\rm corona}\,(R_{\rm g})$	$kT_{\rm e}$ (keV)	τ	Γ	$f_{\rm pl}$
M1	0.049	1.38×10^8	1	60 ± 5	$0.17^{+0.03}_{-0.02}$	21 ± 2	1.80 ± 0.02	0.52 ± 0.02
M2	0.23	1.15×10^8	1	42^{+15}_{-6}	$0.31^{+0.15}_{-0.08}$	13 ± 3	1.87 ± 0.02	0.34 ± 0.04
M3	2.1	1.55×10^7	1	20 ± 3	$0.54^{+0.60}_{-0.23}$	$6.7^{+2.3}_{-5.5}$	2.03 ± 0.02	0.11 ± 0.02
M3	0.77 ± 0.06	$2.6^{+0.4}_{-0.2} \times 10^7$	2.5	12^{+8}_{-2}	$0.26^{+0.29}_{-0.10}$	12^{+11}_{-6}	2.03 ± 0.02	$0.35^{+0.15}_{-0.06}$

1999). The middle spectrum (M2: green) is similar but has a slightly stronger disc component, matching to the mean radio-quiet quasar template of Elvis et al. (1994), but the highest $L/L_{\rm Edd}$ template (M3: red) is very different in terms of shape. It has the lowest 2–10 keV X-ray flux, so these objects are systematically missed in samples based on this energy band. M2 has the highest flux in all observable wavebands, so these are the objects which will be preferentially picked up in optical and X-ray surveys.

We fit the model to the spectral templates to derive the mean parameters. The spectral templates are made by weighting the individual spectra (derived with $f_{\rm col} = 1$) by luminosity distance, whereas the mean mass and $L/L_{\rm Edd}$ quoted in J11b is unweighted. Hence the best-fitting system parameters for the template spectra can differ slightly from those of J11b. Since black hole mass and mass accretion rate are degenerate, we fix the black hole mass to the unweighted mean values of J11b. The dispersion in mass accretion rate is smallest for M2 (J11b), so we fix $L/L_{\rm Edd} = 0.23$ for M2, and normalize all the other spectra to this to derive the best-fitting mean $L/L_{\rm Edd}$ for M1 and M3. These are only slightly different to the mean values given in J11b. Table 3 gives all the resulting parameters.

We then assess the impact of a colour temperature correction. M3 has a maximum disc temperature of 2.5×10^5 K, so we use equation (1) to predict $f_{\rm col} = 2.5$ in the scattering dominated regime, i.e. above $T_{\rm scatt} = 10^5$ K. M1 and M2 are similar in mass and mass accretion rate to the spectra shown in Fig. 1(b), so should have $f_{\rm col} \sim 1.8$ and 2.0, respectively, above $T_{\rm scatt} = 4 \times 10^4$ K. The majority of the disc emission has $T < T_{\rm scatt}$, so this only affects the inner disc. However, in our model the energy from the inner disc is required to power the X-ray emission, so will not be emitted as a blackbody. The considerable X-ray luminosity requires $r_{\rm corona}$ to be substantially larger than the innermost stable orbit, which reduces the maximum disc temperature. Thus the colour temperature correction has little or no effect on these spectra, so we only explore its effect on M3.

We refit M3 with $f_{\rm col} = 2.5$ for $T > 10^5$ K, using the same distance as before, ignoring the unobservable 0.01–0.3 keV region. Guided by the results of Section 4 we allow both mass and mass accretion rate to be free parameters. Again we find that the black hole mass increases and mass accretion rate decreases, giving a mean $L/L_{\rm Edd} = 0.8$ rather than 2.1 as found for $f_{\rm col} = 1$, but all other parameters are consistent with their previous values (see last row of Table 3).

Since the model is based on physical parameters, we can reset the black hole mass to the same value to explore the impact of changing $L/L_{\rm Edd}$ alone. We choose a fiducial mass of $10^8\,{\rm M}_\odot$ (very similar to that of M1 and M2) and set the mass accretion rate to give the same $L/L_{\rm Edd}$ as that derived for each of the spectra in Table 3 (using the parameters from the colour temperature corrected fits to M3). The solid lines in Fig. 8(b) show the resulting evolution of spectral shape in AGN with $L/L_{\rm Edd}$ alone.

The spectral parameters show a clear evolution with increasing $L/L_{\rm Edd}$, most obviously with $r_{\rm corona}$ decreasing, while the 2–10 keV spectral index increases. Changes in the other parameters are not so large, but there is a systematic increase in temperature of the soft excess component, together with a correlated decrease in optical depth so that its spectrum steepens. The amount of power in the soft excess compared to the higher energy emission drops slightly, but the decrease in $r_{\rm corona}$ means that both hard and soft X-ray components carry a smaller fraction of the bolometric luminosity (see also Vasudevan & Fabian 2007).

7 ANALOGY WITH BLACK HOLE BINARY SYSTEMS

BHB shows (at least) three different states, variously termed the low/hard, high/soft (also known as thermal dominant or disc dominant) and very high (also known as steep power-law state). Spectra from this latter state appear very similar to intermediate spectra seen as the source makes a transition from the low/hard to high/soft states (e.g. Belloni et al. 2005). It is plain from Fig. 8(b) that the highest $L/L_{\rm Edd}$ spectrum of M3 is very much like a disc-dominated high/soft state spectrum with a small amount of additional soft Comptonization. The lower luminosity spectra are more ambiguous, and could be either low/hard state spectra or intrinsically steeper very high state spectra which are modified by complex absorption/reflection. We explore each of these possibilities below, and then discuss how we can distinguish between the two scenarios.

7.1 AGN sequence as a low/hard to high/soft transition

The increasing dominance of the disc with increasing $L/L_{\rm Edd}$, together with the switch from hard to soft 2–10 keV X-ray emission is initially very reminiscent of the spectral transition seen in stellar mass galactic BHB systems. These show a clear switch from a hard power law dominated low/hard state to disc dominated high/soft state with a steep tail to higher energies (see e.g. the reviews by McClintock & Remillard 2006, hereafter MR06; DGK07). This is generally interpreted as a decreasing transition radius between a cool disc and hot Comptonized region (Esin, McClintock & Narayan 1997), matching the decreasing $r_{\rm corona}$ seen in our AGN fits.

The BHB in the low/hard state also often show a complex continuum, with a softer Comptonization component from the outer parts of the flow which intercept more seed photons from the disc, together with a harder tail from the hotter central regions (Ibragimov et al. 2005; Makishima et al. 2008; Takahashi et al. 2008; Kawabata & Mineshige 2010). This inhomogeneous Comptonization in BHB is also required to explain the time lags seen in the data (Kotov, Churazov & Gilfanov 2001; Arévalo & Uttley 2006). Thus the two component (soft and hard) Comptonization required to fit the X-ray spectra in M1 and M2 could be analogous to the two component Comptonization spectra seen in the BHB low/hard state.

However, there are also some significant differences. The transition in BHB occurs at $L/L_{\rm Edd} \sim 0.02$ when the mass accretion rate is slowly declining, (Maccarone 2003). This is as expected for an advection-dominated flow, which collapses when the energy transfer between the ions and electrons becomes efficient. The collapse

depends only on optical depth of the flow rather than black hole mass, so should be the same for both AGN and BHB (Narayan & Yi 1995). Yet in these AGN the low/hard state must persist up to at least $L/L_{\rm Edd} \sim 0.2$ to explain M2. Such high transition luminosities are only seen in BHB during the rapid rise during disc outbursts (see e.g. the compilation by Yu & Yan 2009) which drive the flow out of its equilibrium states (Gladstone et al. 2007). Our M2 spectrum would then be analogous to the intermediate state seen during this transition, but this transition is very rapid in BHB so these intermediate spectra are rare (Dunn et al. 2010). By contrast, M2 is very similar to the mean quasi-stellar object (QSO) spectral template of Elvis et al. (1994). and has similar mass and mass accretion rate as a typical QSO (Kollmeier et al. 2006; Steinhardt & Elvis 2010) so it must be a very common state. Thus it does not seem very likely that all these AGN are preferentially seen during a dramatic rise in mass accretion rate. The only real possibility for this AGN sequence to represent a low/hard to high/soft transition is if there is some weak mass dependence on the critical luminosity not predicted by the advective flow models (Narayan & Yi 1995).

7.2 AGN sequence as high mass accretion rate transition

This motivates us to explore the alternative possibility, that the AGN spectra seen here are above the low/hard state transition luminosity, so correspond to one of the high mass accretion states in BHB. The hard X-ray tail ($\Gamma < 2$) is incompatible with this, as these high mass accretion states in BHB almost always have $\Gamma > 2$ (DGK06; MR06). Hence the observed hard X-ray spectra in M1 and M2 would have to be distorted by complex absorption and/or reflection, whereas M3 already has a soft 2–10 keV spectrum, so does not require complex absorption. This potential difference is supported by the behaviour of the soft X-ray excess. In the highest $L/L_{\rm Edd}$ spectra (M3 and RE J1034+396) the soft excess appears as a true excess over a $\Gamma = 2$–2.2 extrapolation of the 10 keV flux level down below 2 keV, unlike M2, M1 and PG 1048+231 where the νf_ν flux level at 0.1 keV is roughly similar to that at 10 keV. The soft excess seen in the highest $L/L_{\rm Edd}$ spectra could then represent a 'true' soft X-ray excess connected to the disc as its approaches Eddington (perhaps bulk motion Comptonization from turbulence; Socrates et al. 2004, or trapped radiation advected along with the flow which can then be released in the plunging region; Sądowski 2009), while the 'bend' seen in the lower $L/L_{\rm Edd}$ is a 'fake' soft excess, where the apparently hard 2–10 keV spectrum and steeper 0.3–2 keV excess are both distortions from complex absorption and/or reflection.

Complex absorption seems quite likely in an AGN environment, as a UV bright disc is very efficient in producing a strong wind from UV line driving (Proga, Stone & Kallman 2000). The wind should become stronger as $L/L_{\rm Edd}$ increases, which is at first sight inconsistent with the requirement that the spectral distortion is larger in M1 and M2 than in M3. However, the wind also depends strongly on black hole mass as it is launched from the region where the disc temperature is around the energies of the strong UV resonance lines, as this is where the opacity peaks. The increase in UV opacity for a lower temperature (i.e. higher mass, lower $L/L_{\rm Edd}$) disc may more than compensate for the lower $L/L_{\rm Edd}$. The wind mass-loss rate may even be substantial enough to modify the disk structure, significantly reducing the mass accretion rate below the wind launching point. We caution that this may require new disc models, which allow the mass accretion rate to change with radius.

The fraction of luminosity emitted in the inferred $\Gamma \sim 2.2$ tail is substantial in both M1 and M2. These spectra would then correspond to the very high/steep power law state seen in BHB (e.g. DK06), whereas M3 would still be a disc-dominated state with a small additional Comptonization component.

However, the M1/M2 spectra do not appear to be modified by complex X-ray absorption. While the signal-to-noise ratio in PG 1048+213 is not overwhelming, this spectrum (Fig. 7) is very similar to the much better data from Mrk 509 which has similar mass and mass accretion rate (Mehdipour et al. 2011; Noda et al. 2011). Here the 'soft excess' clearly has different variability to the 'power law', supporting a true two-component interpretation of the spectrum (Noda et al. 2011). It is the higher mass accretion rate, low-mass objects (more like M3) for which the complex spectral variability is most often interpreted in terms of reflection and/or complex absorption (Fabian et al. 2002, 2009; Miller et al. 2007, 2009, 2010; Turner et al. 2007; Ponti et al. 2010).

7.3 Distinguishing between a low/hard and very high state

The shape of the power spectra of the rapid X-ray variability correlates with spectral state in BHB. However, both low/hard and very high states have variability power spectra which can be roughly characterized as band-limited noise, i.e. have power spectra with both a low- and high-frequency break (see e.g. MR06; DGK07). Conversely, stationary high/soft states (in Cyg X-1) show only a high-frequency break (e.g. MR06; DGK07). Thus both possibilities predict that the objects contributing to M2 should predominantly have power spectra which are band-limited noise, while those which contribute to M3 should extend unbroken to low frequencies. Currently there are no objects in our samples with well-defined variability power spectra, but objects with similar $L/L_{\rm Edd}$ to those in M2/M3 typically show only a high-frequency break, i.e. are more similar to the high/soft state in Cyg X-1 (see e.g. the review by McHardy 2010). However, we caution that if M1 and M2 do indeed correspond to very high state spectra, distorted by complex absorption/reflection, then their variability will also be similarly distorted. Variable obscuration in a clumpy absorber will add to the intrinsic variability, changing the shape and/or normalization of the power spectrum. Even in the reflection model there are differences in predicted variability from the more neutral reflection seen in AGN compared to the much higher ionization expected for the hotter discs in BHB (Done & Gardner, in preparation).

The only clear-cut distinction may be the high-energy spectral shape since this should be much less affected by atomic processes. Low/hard state spectra are intrinsically hard up to a thermal Comptonization rollover at a few hundred keV (e.g. Ibragimov et al. 2005; Makishima et al. 2008; Takahashi et al. 2008), while the high/soft and very high states are soft and extend unbroken beyond 511 keV (Gierliński et al. 1999; Zdziarski et al. 2001; Gierliński & Done 2003). We already know that local AGN do show hard spectra in the 20–200 keV band, with a clear high-energy rollover (Zdziarski et al. 1995), but these have mean luminosity below M1, so clearly correspond to a low/hard state (Vasudevan et al. 2009). Currently there are no objects in our sample with well-defined high-energy spectra. Sensitive higher energy data from *NuSTAr* or *ASTRO-H* on the objects in the M1/M2 sample should give a clear test of their spectral state.

8 CONCLUSIONS

We explore the impact of the accretion disc temperature on the appearance of an AGN. A standard disc model has a maximum temperature $T^4_{\rm max} \propto (L/L_{\rm Edd})/M$ i.e. increases with increasing $L/L_{\rm Edd}$ and with decreasing black hole mass. However, this temperature

assumes that the radiation can completely thermalize, which is not always the case. We follow the approach commonly used in BHB systems and approximate results from full radiative transfer calculations with a colour temperature corrected blackbody. We show that this colour temperature correction is substantial, with $f_{\rm col} \sim 2.5$ for AGN with $T_{\rm max} > 10^5$ K, i.e. well above the temperature at which both H and He are fully ionized so that electron scattering completely dominates the opacity. The colour temperature correction is progressively smaller for lower temperature AGN discs, becoming negligible for $T_{\rm max} < 3 \times 10^4$ K where H starts to become neutral so the associated absorption edge opacity is large. The increase in colour temperature correction with $T_{\rm max}$ leads to an observed maximum disc temperature which increases much faster than predicted from purely blackbody models. This increases the distinction in EUV and hence emission-line properties between objects with low $(L/L_{\rm Edd})/M$ (typically BLS1s) and those with high $(L/L_{\rm Edd})/M$ (typical NLS1s).

We show that the colour temperature correction is large enough that the disc extends into the soft X-ray bandpass in the lowest mass/highest mass accretion rate AGN such as the extreme NLS1 RE J1034+396. For these systems, much of the soft X-ray emission is directly produced by the accretion disc unless the disc structure is very different to that predicted. However, the shape of the disc emission does not match that of the observed 'soft X-ray excess' but requires Compton upscattering to be important.

We assume that this Comptonization takes place in the disc itself rather than in a separate corona, a scenario which is supported by the lack of variability seen in this component in some extreme NLS1 (Jin et al. 2009; Middleton et al. 2009). We build a self-consistent model for this, assuming that the disc structure changes inside some radius $r_{\rm corona}$, so the energy emitted within this emerges as Compton upscattering rather than being able to thermalize to a (colour temperature corrected) blackbody. We include the higher energy emission (power-law tail) in our model by assuming that part of the Compton upscattering takes place in a hot, optically thin corona above and below the inner disc while the remainder is dissipated in the disc itself, but emerges as low temperature/optically thick Comptonized emission rather than as a blackbody. The key new aspect of our model is that the luminosity of the soft excess and tail are constrained by energy conservation as we assume that all the material accretes through the outer thin disc.

The model fits well to the extreme NLS1 spectra, where there is a 'true' soft X-ray excess component seen above a weak X-ray tail which has $\Gamma \sim 2$–2.2. The majority of the emission in these objects is dissipated in the optically thick disc, with only ∼15 per cent of the bolometric flux required to form the soft X-ray excess, and 10 per cent producing the high-energy tail. The small amount of energy in the soft and hard Comptonization components gives an implied $r_{\rm corona} \sim 10$–$20R_{\rm g}$. At lower mass accretion rates we might expect that the disc remains able to thermalize down to lower radii, so that the spectra become even more disc dominated. However, the opposite is true if the spectra are indicative of the intrinsic emission. Another issue with these spectra are that they appear rather similar to the low/hard state in BHB, yet are seen up to $L/L_{\rm Edd} \sim 0.2$, a factor 10 higher than expected from BHB. This would indicate some process which breaks the mass scaling from BHB to AGN.

Instead, multiple authors have suggested that the soft excess and apparently hard 2–10 keV spectra arise as result of complex absorption and/or reflection. If this is the case, the variability power spectra will also be distorted, as clumpy absorption adds to the intrinsic variability, as does the more neutral reflection expected in an AGN. However, while the highest $L/L_{\rm Edd}$ spectra do show complex, energy dependent variability which may well indicate that these processes shapes the spectrum, the lower $L/L_{\rm Edd}$ objects, where the soft excess component is most important in terms of the fraction of bolometric luminosity, do not. The soft excess and hard spectra in these objects appear instead to be intrinsic. Since these features are not seen in BHB at these $L/L_{\rm Edd}$ then this does require an additional process to break the mass scaling from BHB to AGN.

Extending the spectra beyond 10 keV with *Suzaku*, *NuStar* and *Astro-H* may give the only clear-cut test of the correspondence between AGN and BHB states.

ACKNOWLEDGMENTS

We thank our referee, Bozena Czerny, for detailed comments and questions which clarified our discussion of the colour temperature correction in AGN discs. CD acknowledges illuminating conversations on the correspondence between AGN and BHB with Ian McHardy and Phil Uttley.

REFERENCES

Abramowicz M. A., Czerny B., Lasota J. P., Szuszkiewicz E., 1988, ApJ, 332, 646
Arévalo P., Uttley P., 2006, MNRAS, 367, 801
Arnaud K. A., 1996, in Jacoby G., Barnes J., eds, ASP Conf. Ser. Vol. 101, Astronomical Data Analysis Software and Systems V. Astron. Soc. Pac., San Francisco, p. 17
Balbus S. A., Hawley J. F., 1991, ApJ, 376, 214
Bechtold J., Czerny B., Elvis M., Fabbiano G., Green R. F., 1987, ApJ, 314, 699
Belloni T., Homan J., Casella P., van der Klis M., Nespoli E., Lewin W. H. G., Miller J. M., Méndez M., 2005, A&A, 440, 207
Blaes O., Krolik J. H., Hirose S., Shabaltas N., 2011, ApJ, 733, 110
Boller T., Brandt W. N., Fink H., 1996, A&A, 305, 53
Casebeer D. A., Leighly K. M., Baron E., 2006, ApJ, 637, 157
Chevallier L., Collin S., Dumont A.-M., Czerny B., Mouchet M., Gonçalves A. C., Goosmann R., 2006, A&A, 449, 493
Crummy J., Fabian A. C., Gallo L., Ross R. R., 2006, MNRAS, 365, 1067
Czerny B., Elvis M., 1987, ApJ, 321, 305
Czerny B., Nikołajuk M., Różańska A., Dumont A.-M., Loska Z., Zycki P. T., 2003, A&A, 412, 317
Davis S. W., Hubeny I., 2006, ApJS, 164, 530
Davis S. W., Laor A., 2011, ApJ, 728, 98
Davis S. W., Blaes O. M., Hubeny I., Turner N. J., 2005, ApJ, 621, 372
Davis S. W., Done C., Blaes O. M., 2006, ApJ, 647, 525
Done C., 2010, preprint (arXiv:1008.2287)
Done C., Davis S. W., 2008, ApJ, 683, 389
Done C., Kubota A., 2006, MNRAS, 371, 1216
Done C., Gierliński M., Kubota A., 2007, A&AR, 15, 1 (DGK07)
Dunn R. J. H., Fender R. P., Körding E. G., Belloni T., Cabanac C., 2010, MNRAS, 403, 61
Elvis M. et al., 1994, ApJS, 95, 1
Esin A. A., McClintock J. E., Narayan R., 1997, ApJ, 489, 865
Fabian A. C., Ballantyne D. R., Merloni A., Vaughan S., Iwasawa K., Boller T., 2002, MNRAS, 331, L35
Fabian A. C. et al., 2009, Nat, 459, 540
Fanidakis N. et al., 2011, MNRAS, 410, 53
Gierliński M., Done C., 2003, MNRAS, 342, 1083
Gierliński M., Done C., 2004, MNRAS, 349, L7
Gierliński M., Zdziarski A. A., Poutanen J., Coppi P. S., Ebisawa K., Johnson W. N., 1999, MNRAS, 309, 496
Gladstone J., Done C., Gierliński M., 2007, MNRAS, 378, 13
Grupe D., Wills B. J., Leighly K. M., Meusinger H., 2004, AJ, 127, 156
Hubeny I., Blaes O., Krolik J. H., Agol E., 2001, ApJ, 559, 680
Hure J.-M., Collin-Souffrin S., Le Bourlot J., Pineau des Forets G., 1994, A&A, 290, 19

Ibragimov A., Poutanen J., Gilfanov M., Zdziarski A. A., Shrader C. R., 2005, MNRAS, 362, 1435
Janiuk A., Czerny B., Madejski G. M., 2001, ApJ, 557, 408
Jin C., Done C., Ward M., Gierliński M., Mullaney J., 2009, MNRAS, 398, L16
Jin C., Ward M., Done C., Gelbord J., 2011a, MNRAS, in press (doi:10.1111/j.1365-2966.2011.19805.x) (this issue) (J11a)
Jin C., Ward M., Done C., Gelbord J., 2011b, MNRAS, submitted (J11b)
Kaspi S., Smith P. S., Netzer H., Maoz D., Jannuzi B. T., Giveon U., 2000, ApJ, 533, 631
Kawabata R., Mineshige S., 2010, PASJ, 62, 621
Kollmeier J. A. et al., 2006, ApJ, 648, 128
Koratkar A., Blaes O., 1999, PASP, 111, 1
Kotov O., Churazov E., Gilfanov M., 2001, MNRAS, 327, 799
Kubota A., Makishima K., Ebisawa K., 2001, ApJ, 560, L147
Kubota A., Done C., 2004, MNRAS, 353, 980
Laor A., Fiore F., Elvis M., Wilkes B. J., McDowell J. C., 1997, ApJ, 477, 93
Maccarone T. J., 2003, A&A, 409, 697
McClintock J. E., Remillard R. A., 2006, in Lewin W., van der Klis M., eds, Cambridge Astrophys. Ser. 39, Compact Stellar X-Ray Sources. Cambridge Univ. Press, Cambridge, p. 157 (MR06)
McHardy I., 2010, in Lecture Notes in Physics, Vol. 794, The Jet Paradigm. Springer-Verlag, Berlin, p. 203
Magdziarz P., Blaes O. M., Zdziarski A. A., Johnson W. N., Smith D. A., 1998, MNRAS, 301, 179
Magorrian J. et al., 1998, AJ, 115, 2285
Makishima K. et al., 2008, PASJ, 60, 585
Mehdipour M. et al., 2011, A&A, in press (arXiv:1107.0659)
Middleton M., Done C., Ward M., Gierliński M., Schurch N., 2009, MNRAS, 394, 250
Miller L., Turner T. J., Reeves J. N., George I. M., Kraemer S. B., Wingert B., 2007, A&A, 463, 131
Miller L., Turner T. J., Reeves J. N., 2009, MNRAS, 399, L69
Miller L., Turner T. J., Reeves J. N., Braito V., 2010, MNRAS, 408, 1928
Narayan R., Yi I., 1995, ApJ, 452, 710
Noda H., Makishima K., Yamada S., Torii S., Sakurai S., Nakazawa K., 2011, PASJ, in press (arXiv:1109.0457)
Novikov I. D., Thorne K. S., 1973, in Dewitt C., Dewitt B. S., eds, Black Holes. Gordon & Breach, New York, p. 343
Nowak M. A., 1995, PASP, 107, 1207
Ponti G. et al., 2010, MNRAS, 406, 2591
Proga D., Stone J. M., Kallman T. R., 2000, ApJ, 543, 686
Puchnarewicz E. M., Mason K. O., Siemiginowska A., Fruscione A., Comastri A., Fiore F., Cagnoni I., 2001, ApJ, 550, 644
Risaliti G., Nardini E., Salvati M., Elvis M., Fabbiano G., Maiolino R., Pietrini P., Torricelli-Ciamponi G., 2011, MNRAS, 410, 1027
Ross R. R., Fabian A. C., Mineshige S., 1992, MNRAS, 258, 189
Sądowski A., 2009, ApJS, 183, 171
Sani E., Lutz D., Risaliti G., Netzer H., Gallo L. C., Trakhtenbrot B., Sturm E., Boller T., 2010, MNRAS, 403, 1246
Schurch N. J., Done C., 2007, MNRAS, 381, 1413
Shakura N. I., Sunyaev R. A., 1973, A&A, 24, 337
Shimura T., Takahara F., 1995, ApJ, 445, 780
Sim S. A., Miller L., Long K. S., Turner T. J., Reeves J. N., 2010, MNRAS, 404, 1369
Socrates A., Davis S. W., Blaes O., 2004, ApJ, 601, 405
Steinhardt C. L., Elvis M., 2010, MNRAS, 402, 2637
Takahashi H. et al., 2008, PASJ, 60, S69
Titarchuk L., 1994, ApJ, 434, 570
Turner T. J., Miller L., Reeves J. N., Kraemer S. B., 2007, A&A, 475, 121
Vasudevan R. V., Fabian A. C., 2007, MNRAS, 381, 1235
Vasudevan R. V., Mushotzky R. F., Winter L. M., Fabian A. C., 2009, MNRAS, 399, 1553
Yu W., Yan Z., 2009, ApJ, 701, 1940
Zdziarski A. A., Johnson W. N., Done C., Smith D., McNaron-Brown K., 1995, ApJ, 438, L63
Zdziarski A. A., Johnson W. N., Magdziarz P., 1996, MNRAS, 283, 193
Zdziarski A. A., Grove J. E., Poutanen J., Rao A. R., Vadawale S. V., 2001, ApJ, 554, L45
Zhang S. N., Cui W., Chen W., 1997, ApJ, 482, L155

APPENDIX A: COMPARISON OF OPTXAGN WITH DKBBFTH

DK06 developed such a similar model (DKBBFTH) in which the Comptonization is energetically coupled to the accretion flow. This was applied to the very high state of Galactic BHB, where the disc is strongly Comptonized by optically thick ($\tau \sim 2$–3) plasma which has a lower temperature ($kT \sim 20$ keV) than the typical temperatures of 100–200 keV seen at lower luminosity. DK06 assumed that the Comptonizing corona formed a homogeneous plane-parallel

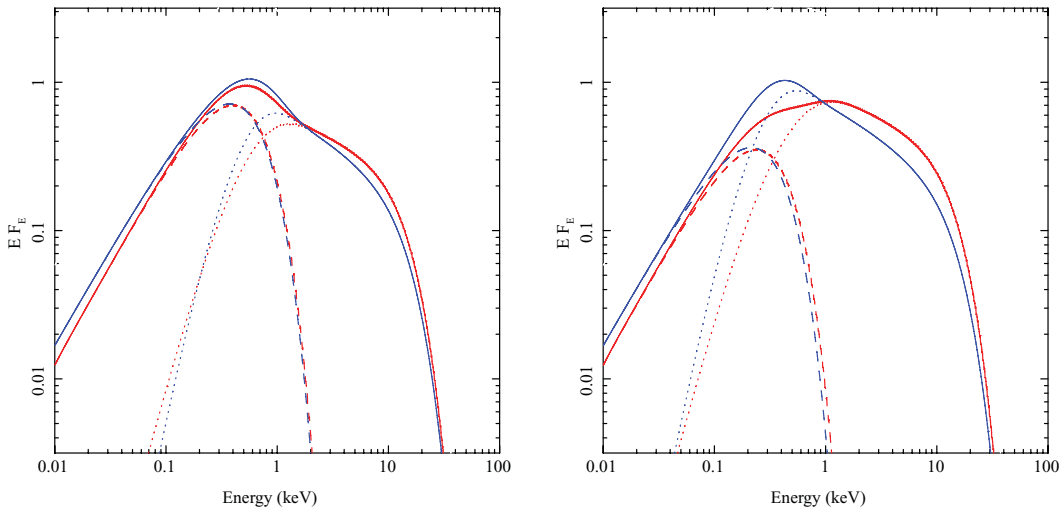

Figure A1. Comparison of DK06 (red) and this model (blue) for (a) 50 and (b) 75 per cent of the total accretion power being Comptonized rather than radiated as a blackbody. The solid line shows the total model spectrum, which is made up of the outer disc (dashed line) and inner Comptonized emission (dotted line). The outer disc emission is always very similar, while the Comptonized emission can be different due to the different assumptions about the seed photon energies. However, this only gives a significant difference where most of the accretion power is Comptonized (as in b).

atmosphere above the disc below some characteristic radius $r_{\rm corona}$, and that it is directly powered by accretion. Above this radius the disc emits all the energy dissipated by gravity as a blackbody at the local temperature. Below this, the energy is split between the optically thick disc and corona. More energy dissipation in the corona implies less energy dissipated in the optically thick disc, so its luminosity and temperature is lower. The local disc photons act as the source of seed photons for the Comptonization, so the Comptonization has to be done locally at many annuli in the corona as this seed photon temperature varies with radius. This makes the DK06 model extremely slow, so it is not feasible to use it to fit a large sample of spectra.

Instead we develop a much faster model which keeps the key aspect of energy conservation. We simply assume that the energy within $r_{\rm corona}$ is emitted as Compton upscattered flux, with seed photons characterized by a blackbody at the disc temperature at $r_{\rm corona}$. We also replace the underlying Newtonian emissivity ($L(r) \propto r^{-3}$) used by DK06 with the fully relativistic Novikov–Thorne dissipation.

We explicitly compare of our new model (blue) with that of DK06 (red) in Fig. A1. We assume a Schwarzschild black hole of $10\,{\rm M}_{\odot}$, accreting at $L/L_{\rm Edd} = 0.04$. This gives a maximum disc temperature of 0.29 keV, so we use this as the peak temperature of the DK06 model and normalize the models so they have the same flux. Fig. A1(a) shows a comparison between the two models for the case where 50 per cent of the accretion power is dissipated below $r_{\rm corona}$ (i.e. $12R_{\rm g}$ for DK06, compared to $30R_{\rm g}$ in the fully relativistic emissivity), while Fig. A1(b) is for 75 per cent of the accretion power (i.e. $24R_{\rm g}$ for DK06, compared to $75R_{\rm g}$ in the fully relativistic emissivity). The blackbody outer disc and Comptonized inner disc components of each model are shown as a dashed and dotted line, respectively. The difference in radial emissivity gives a slightly different shape to the disc emission for pure blackbody spectra which is the reason for the slightly different normalization of the outer disc emission at low energies. As discussed above, the two models are very similar except for the seed photon energy for the Comptonized emission. This only makes a noticeable difference if most of the power is dissipated in the Comptonization region (i.e. $r_{\rm corona} \geq 75R_{\rm g}$), and most of this difference is confined to the unobservable EUV region. However, this does allow the accretion energy to peak at a lower temperature than the equivalent thermalized emission, which is probably unphysical, so we urge caution in interpretating the parameters when large $r_{\rm corona}$ are derived together with steep soft X-ray Comptonized spectra.

In all other circumstances this new model incorporates energy conservation in the same way as DKBBFTH and gives results which are very similar, yet is much faster so it is feasible to fit multiple spectra.

This paper has been typeset from a TEX/LATEX file prepared by the author.